

Numerical Solution of Micropolar Fluid Flow with Zero Mass Flux of Nanoparticles at Stretching Surface with a Porous Medium

Rizwan Ul Haq^{1,*} and Adara M. Blaga²

¹ School of Natural Sciences (SNS), National University of Science and Technology (NUST), H-12, Islamabad 44000, Pakistan

² Department of Mathematics, Faculty of Mathematics and Computer Science, West University of Timisoara, 300223 Timisoara, Romania

Abstract. This paper investigates the comprehensive investigation of mixed convection flow and heat transfers analysis of Micropolar by considering porous medium and heat absorption. Subsequently, mathematical formulation was modeled using boundary conditions. Two major aspects, Brownian motion and thermophoresis are addressed in the energy and concentration equation which are coupled with momentum equation. By using similarity variables, the entire system of partial differential equations govern through momentum, energy, angular momentum and concentration are converted into system of nonlinear ordinary differential equations. Nonlinear systems are solved by using numerical approach with `bvp4c` function in MATLAB that is based on the collocation method, specifically the three-point Lobatto IIIa formula is directed to type of finite difference method. Results are obtained for various emerging parameters. It has been observed that skin friction decreases for increasing values of Hartmann number and Eckert number. Decreasing trend of bar graphs is observed against Nusselt number and Sherwood number against Brownian motion and thermophoresis parameters.

AMS subject classifications: 65L06, 34C20

Key words: Zero mass flux, Heat transfer, Nanofluid, Boundary layer flow, Mixed convection, Numerical solution.

*

1 Introduction

Research in exceptional areas has been offered by fluid mechanics. The continuing advancement of fluid mechanics theory and applications has been facilitated by

*Corresponding author. Email addresses: r.haq.qau@gmail.com (R. U. Haq).

©2024 by the author(s). Licensee Global Science Press. This is an open access article distributed under the terms of the Creative Commons Attribution (CC BY) License, which permits unrestricted use, distribution, and reproduction in any medium, provided the original author and source are credited.

researchers. The most deep-rooted model of Navier-Stokes for classical fluids presents that the motions of Newtonian fluids seem to be incompressible. Nevertheless, Navier-Stokes representation is insufficient to explain liquids like polar fluids, fluids with microstructural components. These fluids are fascinating on their own and essential from a practical one. Most of these consisting of the Polymeric suspensions, blood of animals, crystals of liquid characterize these fluids that are complex. Their constituent particles could enlarge and contract, their shapes might vary, and they can rotate independently.

Several explanations have been proposed, even though basic deformable directed fluids, simple microfluid theories, and dipolar fluids all resemble the type of fluids containing microstructure. Eringen [1, 2] was the first to put out the theory of micro fluids, which thoroughly investigates the Navier-Stokes model. The microscopic movement and local structure for the fundamental elements of fluid are associated with microscopic effects that have been seen in micro fluids. Spin inertia has an impact on such fluids, which can withstand tension and bodily movements. Eringen [3] then advanced the notion of micropolar fluids. This theory contains established fluid medium that is under stress along with micro rotational effects, micro rotational inertia, and a couple stresses. He examined flow problems of one-dimensional micropolar fluids. He worked on one-dimensional micropolar fluid flow problems. Furthermore particular, he examined the uniform flow of micropolar fluids in different channels like ducts, tubes, circular, and spherical. Specifically, and presented graphical representations for coupled stress, shear stress differences, velocity, and micro-rotation profiles.

Physically, this category of bar-like elements in the same approach as the fluids that are isotropic fluids, e.g., crystals of liquids, that together with molecules resembling dumbbells, blood of animals, fluids containing polymers and those fluids which have additives. This theory has been predicted to also offer a mathematical explanation for non-Newtonian behavior seen in some synthetic liquids, such blood and polymers. Fundamental flow problems have been studied using Micropolar Fluid concepts framework. The research conducted in the field of micropolar fluid flow problems as well as its possible applications was first described by Ariman et al. [4, 5]. Turk et al. [6, 7], Hogen et al. [8], and Lee et al. [9] have tackled the blood flow models. In contrast, Allen et al. [11] proposed the idea of a lubrication of micropolar fluids. Tozeren et al. [10] used the concept of micropolar fluids for suspension.

Making use of a finite difference method, Chapman and Bauer [12] were successful in finding a group of accurate solutions to the Navier-Stokes equations. For micropolar instance, this issue was investigated Agarwal [13], Takhar, and Soundalgekar [13,14] discussed the flow and heat transport of both micropolar fluids over a porous medium. Mathur and Ena [15] investigated laminar convective boundary layer flow for a thermo-micropolar fluid using a non-isothermal vertical flat plate. A class of accurate solutions for the Magneto hydrodynamics flow for micropolar fluids trapped between parallel, non-coaxial, insulated, and infinite spinning discs were studied by Kasiviswanathan and Gandhi [16]. Lange [17], Guram and Smith [18] researched an accurate solution for the uniform Magneto hydrodynamics flow for a micropolar fluid examined, together with the stationary flow for micropolar fluids with powerful and fragile contact.

Al-Sanea [19] examined mixed convection heat transfer with a constantly rotating heated vertical channel by investigating at suction or injection. Kumari and Nath [20] examined mixed convection boundary layer flow across a confined vertical cylinder along concentrated injection or suction and cooling or heating. Outside of a stretched empty cylinder, Wang [21] studied the flow in an acoustic fluid at rest that was viscous and incompressible. The effects of a shrinking sheet on Magneto hydrodynamic viscous flow were examined by Sajid and Hayat [22] using the homotopy analysis method. Sajid et al. [23] explored the magneto hydro-dynamic rotating flow of a viscous fluid over a contracting surface. To analyze Magneto hydrodynamics flow for non-Newtonian fluid across stretched sheet, Liao [24] developed an analytical solution. The two-dimensional boundary layer was examined by Vajravelu [25] and Tsai et al. [26] due to the non-uniform stretching surface. Ishak et al. [27] examined the effects for a constant hydrostatic pressure of flow and heat transfer outside a stretched porous cylinder and used the Keller-box technique for numerical solutions. Wang [28] investigated the stagnation flow in the direction of a contracting plate. According to his discussions the axisymmetric and two-dimensional examinations of this study are under consideration. A unique class of solutions with exact similarity and reverse flow was examined in his study. Fang and Zhang [29] examined magneto hydrodynamics flow along a shrinking surface and provided an accurate solution to the problem. Khan and Pop [30] proposed a nanofluid model based upon Brownian motion and thermophoresis coupled with concentration and energy equations over a stretched flat surface.

Rahman et al. [31] conducted computational modeling to study the effect of fluid electric conductivity and non-uniform source of heat or sink to a two-dimensional, uniform, hydromagnetic, and convective flow for a micropolar fluid in contrast to fluid layer flow with a slanted solid surface with a homogeneous surface heat flux. Hayat et al. [32] studied the two-dimensional Magnetohydrodynamics unsteady flow for an incompressible micropolar fluid through a nonlinear stretching sheet. Ishak et al. [33] examined the continuous Magnetohydrodynamics mixed convection stagnation flow for a vertical surface immersed in an incompressible micropolar fluid. Ishak et al. [34] investigated the stagnation flow for magnetohydrodynamics boundary layer flow in the presence of a changing magnetic field using a spike with a constant flux of surface heat covered in an incompressible micropolar fluid. The constant convective heat transfer boundary layer movement for a vertical surface immersed in an incompressible micropolar fluid is taken into consideration by Ishak et al [35] in the analysis. El-Mistikawy [36] investigated flow through the boundaries of a micro-polar fluid caused by continuously extended surface in the case of decreasing coupled variables. Kumaran et al. [37] accurately solve for mixed convection flow for a liquid along an electrical conductivity through a nonlinearly extended and linear transparent surface. Nazar et al. [38] have investigated the movement of an incompressible micropolar fluid with the presence at a stable, two-dimensional stagnation flow when the sheet is extended inside the field with a speed proportionate the distance from the stagnation point. Noor et al. [39] examined micropolar fluid flow along a vertically moving surface.

Examining numerical solution of Micropolar fluids due to moving surfaces is the objective of this study. In Section 2 we have defined the mathematical model that is based upon energy, momentum, angular momentum, and concentration equations. In the same section physical quantity of interest is also defined. In Section 3, methodology to solve the proposed model is defined. A result analysis of each parameter is described in Section 4. In the final Section 5, the major findings of the entire study are described reflecting the behavior of fluid motion and its heat transfer.

2 Mathematical Formulation of the Problem

In this problem, we are considering cartesian coordinate system with a moving surface incompressible, stationary, two-dimensional, micropolar, and nano-fluid laminar flow. Two-dimensional coordinate system is considered to developed the geometry of the model (see Figure 1).

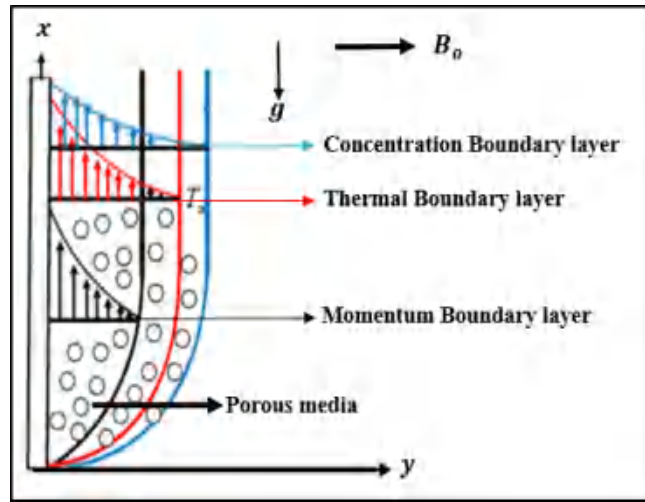


Figure 1: Geometry of the model.

The governing equations that represent boundary layer flow for equations of continuity, momentum, angular momentum, energy, and concentration can be defined by using the approximate boundary conditions:

$$\frac{\partial \tilde{u}}{\partial x} + \frac{\partial \tilde{u}}{\partial y} = 0, \quad (1)$$

$$\rho \left(\tilde{u} \frac{\partial \tilde{u}}{\partial x} + \tilde{v} \frac{\partial \tilde{u}}{\partial y} \right) = (\mu + \kappa) \left(\frac{\partial^2 \tilde{u}}{\partial y^2} \right) + \kappa \left(\frac{\partial \tilde{N}}{\partial y} \right) - \sigma B_0^2 \tilde{u} + \frac{\nu}{\kappa} \pm g \left[\begin{array}{l} \beta_T (T - T_\infty) \\ + \beta_c (C - C_\infty) \end{array} \right], \quad (2)$$

$$\rho j \left(\tilde{u} \frac{\partial \tilde{N}}{\partial x} + \tilde{v} \frac{\partial \tilde{N}}{\partial y} \right) = \gamma \frac{\partial^2 \tilde{N}}{\partial x^2} + \kappa \left(\frac{\partial \tilde{N}}{\partial y} + 2\tilde{N} \right), \quad (3)$$

$$\rho C_p \left(\tilde{u} \frac{\partial \tilde{T}}{\partial x} + \tilde{v} \frac{\partial \tilde{T}}{\partial y} \right) = k \left(\frac{\partial^2 \tilde{T}}{\partial y^2} \right) + (\mu + \kappa) \left(\frac{\partial \tilde{u}}{\partial y} \right)^2 + \sigma B_0^2 \tilde{u}^2 + \frac{(\rho C_p)_p}{(\rho C_p)_f} \left(D_B \frac{\partial \tilde{C}}{\partial y} \frac{\partial \tilde{T}}{\partial y} + \frac{D_T}{D_B} \left(\frac{\partial \tilde{T}}{\partial y} \right)^2 \right) + \frac{Q_0}{\rho c_p} (\tilde{T} - \tilde{T}_\infty), \quad (4)$$

$$\tilde{u} \frac{\partial \tilde{C}}{\partial x} + \tilde{v} \frac{\partial \tilde{C}}{\partial y} = D_B \frac{\partial^2 \tilde{C}}{\partial x^2} + \frac{D_T}{T_\infty} \frac{\partial^2 \tilde{T}}{\partial y^2}. \quad (5)$$

In the above system of equations, \tilde{u} and \tilde{v} are velocities of fluid molecules, \tilde{N} is the angular momentum, \tilde{T} is the temperature and \tilde{C} is the concentration of fluid. Equation (1) represents the conservation of mass know as continuity equation, Equation (2) represents the momentum equation, Equation (3) represents the angular momentum equation, Equation (4) represents the energy equation and Equation (5) represents the concentration equation of fluid molecules. Boundary conditions take the following way:

$$\tilde{u} = bx^* + L\tilde{u}_y, \tilde{v} = 0, \tilde{N} = 0, \tilde{T} = \tilde{T}_w, \tilde{C} = \tilde{C}_w \quad \text{at } \tilde{y} = 0, \tag{6a}$$

$$\tilde{u} = 0, \tilde{N} = 0, \tilde{T} = \tilde{T}_\infty, \tilde{C} = \tilde{C}_\infty \quad \text{at } \tilde{y} \rightarrow \infty. \tag{6b}$$

By introducing the similarity transformation

$$\eta = \sqrt{b/v_f} y, \tilde{u} = bxf'(\eta), \tilde{v} = -\sqrt{bv_f}f(\eta), \tilde{N} = \sqrt{b^3/v_f}xg(\eta), \tag{7a}$$

$$\theta(\eta) = \frac{\tilde{T}-\tilde{T}_\infty}{\tilde{T}_w-\tilde{T}_\infty}, \tilde{T} = \tilde{T}_\infty + Ax\theta(\eta), \phi(\eta) = \frac{\tilde{C}-\tilde{C}_\infty}{\tilde{C}_w-\tilde{C}_\infty}, \tilde{C} = \tilde{C}_\infty + Bx\phi(\eta). \tag{7b}$$

Stream function ψ can be expressed as:

$$\tilde{u} = \tilde{\psi}_y, \quad \tilde{v} = -\tilde{\psi}_x.$$

Making use of these transformations, identically continuity equation is satisfying and Equations (2)–(5) along with the conditions on boundary (7a) and (7b) takes the following expressions:

$$(1 + K)f'''' + ff'' - f'^2 + Kg' - Mf' + \frac{1}{Da}f' \pm Gr_1\theta \pm Gr_2\phi = 0, \tag{8}$$

$$\left(1 + \frac{K}{2}\right)g'' + fg' - f'g - K(2g + f'') = 0, \tag{9}$$

$$\theta'' + Prf\theta' - Prf'\theta + (1 + K)PrEc f''^2 + PrEcMf'^2 + PrNb\theta'\phi' + PrNt\theta'^2 + PrQ\theta = 0, \tag{10}$$

$$\phi'' + Scf\phi' - Scf'\phi + \frac{N_t}{N_b}\theta'' = 0. \tag{11}$$

The parameters of thermophoresis and Brownian motion are defined as

$$N_t = \frac{\tau D_B (\tilde{T}_w - \tilde{T}_\infty)}{v_f \tilde{T}_\infty}, \quad N_b = \frac{\tau D_B (\tilde{T}_w - \tilde{T}_\infty)}{v_f}$$

while the rest of the parameters are defined as

$$M = \frac{\partial B_0^2}{(\rho_f) b}, \quad K = \frac{\kappa_f}{\rho_f v_f}, \quad Da = \frac{\kappa_b}{v},$$

$$Gr_1 = g\beta \left(\frac{\tilde{T}_w - \tilde{T}_\infty}{b^2 x} \right), \quad Gr_2 = g\beta \left(\frac{\tilde{C}_w - \tilde{C}_\infty}{b^2 x} \right),$$

$$Pr = \frac{c_p \mu}{\kappa_\infty}, \quad Ec = \frac{\tilde{u}_w^2}{c_p (\tilde{T}_w - \tilde{T}_\infty)}, \quad Q = \frac{Q_0}{\kappa_f (\rho c_p) f b}.$$

By using similarity transformations (7), conditions (6) take the form

$$f(\eta) = 0, \quad f'(\eta) = 1 + sf''(\eta), \quad \theta(\eta) = \phi(\eta) = 1 \quad \text{at } \eta = 0, \tag{12a}$$

$$f'(\eta) = g(\eta) = \theta(\eta) = \phi(\eta) = 0 \quad \text{at } \eta \rightarrow \infty. \tag{12b}$$

For very small values of slip parameter ($s \approx 0$), surface flux is defined by

$$\tilde{q}_w(x) = -k_f(\tilde{T}_y)_{y=0} = -k_f(\tilde{T}_w - \tilde{T}_\infty)\sqrt{bv_f}\theta'(0), \tag{13}$$

the surface heat flux transfer coefficient can be expressed as

$$\tilde{h}_x = \frac{\tilde{q}_w(x)}{(\tilde{T}_w - \tilde{T}_\infty)}, \quad (14)$$

Nusselt number is written as

$$\tilde{N}u_x = \frac{x\tilde{h}(x)}{k_f(\tilde{T}_w - \tilde{T}_\infty)},$$

or

$$\tilde{N}u_x = \frac{x\tilde{q}_w(x)}{k_f} = -\sqrt{\frac{b}{v_f}} x\theta'(0) \Rightarrow \frac{\tilde{N}u_x}{\sqrt{Re_w}} = -\theta'(0), \quad (15)$$

Sherwood number can be defined as

$$\tilde{S}h_x = \frac{j_w x}{D_f(\tilde{C}_w - \tilde{C}_\infty)} = -\sqrt{\frac{b}{v_f}} x\phi'(0) \Rightarrow \frac{\tilde{S}h_x}{\sqrt{Re_w}} = -\phi'(0). \quad (16)$$

3 Methodology

By employing the built-in `bvp4c` approach after conversion of the given PDEs to the first order ODEs using MATLAB program for the solution. The detailed procedure of this method is mentioned by Noor et al. [39]. For numerical results we have considered

$$\begin{aligned} f &= y_1, & g &= y_4, & \theta &= y_6, & \phi &= y_8, \\ f' &= y_2, & g' &= y_5, & \theta' &= y_7, & \phi' &= y_9, \\ f'' &= y_3, & g'' &= y_{11}, & \theta'' &= y_{12}, & \phi'' &= y_{13}, \\ & & & & f''' &= y_{10}. \end{aligned}$$

Equation (8) becomes

$$(1 + K)y_{10} + y_1y_2 - y_2^2 + Ky_5 - My_2 + \frac{1}{D_a}y_2 \pm Gr_1y_6 \pm Gr_2y_8 = 0,$$

or

$$y_{10} = \frac{1}{1 + K} \left[-y_1y_2 + y_2^2 - Ky_5 + My_2 - \frac{1}{D_a}y_2 \pm Gr_1y_6 \pm Gr_2y_8 \right].$$

Equation (9) becomes

$$\left(1 + \frac{K}{2}\right)y_{11} + y_1y_5 - y_2y_4 - K(2y_4 + y_3) = 0,$$

or

$$y_{11} = 2 \left(\frac{-y_1y_5 + y_2y_4 + K(2y_4 + y_3)}{2 + K} \right).$$

Equation (10) becomes

$$y_{12} + Pr y_1 y_7 + (1 + K)PrEcy_3^2 + PrEcMy_2^2 + PrN_b y_7 y_9 + PrN_t y_7^2 + PrQy_6 = 0,$$

or

$$y_{12} = -Pr y_1 y_7 - (1 + K)PrEcy_3^2 - PrEcMy_2^2 - PrN_b y_7 y_9 - PrN_t y_7^2 - PrQy_6.$$

Equation (11) becomes

$$y_{13} + Scy_1y_9 - Scy_2y_8 + \frac{N_T}{N_b}y_{12} = 0,$$

or

$$y_{13} = -Scy_1y_9 + Scy_2y_8 - \frac{N_T}{N_b}y_{12}.$$

Therefore, we get

$$\begin{bmatrix} f' \\ f'' \\ f''' \\ f'''' \\ g' \\ g'' \\ \theta' \\ \theta'' \\ \phi \\ \phi'' \end{bmatrix} = \begin{bmatrix} y_2 \\ y_3 \\ y_{10} \\ y_5 \\ y_{11} \\ y_7 \\ y_{12} \\ y_9 \\ y_{13} \end{bmatrix} \begin{bmatrix} y_2 \\ y_3 \\ \left(\frac{-y_1y_2 + y_2^2 - Ky_5 + My_2 - \frac{1}{D_a}y_2 \pm Gr_1y_6 \pm Gr_2y_8}{1 + K} \right) \\ y_5 \\ 2 \left(\frac{-y_1y_5 + y_2y_4 + K(2y_4 + y_3)}{2 + K} \right) \\ y_{11} \\ -Pr y_1y_7 - (1 + K)PrEc y_3^2 - PrEcMy_2^2 - PrNb y_7y_9 - PrN_t y_7^2 - PrQy_6 \\ y_9 \\ -Scy_1y_9 + Scy_2y_8 - \frac{N_T}{N_b}y_{12} \end{bmatrix}.$$

4 Results and Discussions

For the sake of the required results of the above boundary value problems, we first transform all the PDEs of momentum, angular momentum, energy, and concentration into non-linear ODEs by similar transformation with their corresponding boundary conditions. One very interesting behavior is observed that the energy equation is being transformed into two cases. The first solution associated with positive (+) part of the eq. (8) represents assisting flow while second solution associated with negative (-) part of eq. (8) represents opposing flow. The results of these two cases are shown in graphs where solid lines indicate assisting flow while dotted lines indicate opposing flow. The effects are apparent for all physical parameters involved and the nonlinear ODEs are illustrated to velocity profile, temperature profile, angular velocity profile, and concentration profiles. The impacts for some of parameters are seen in graphs where the arrow in the figure indicates the increasing/decreasing in assisting flow.

Table 1: Results validation for Nusselt number and the Sherwood number in the absence of Micropolar rotation effects, $K = M = Gr_1 = Gr_2 = Ec = Q = s = Sc = 0$ when $Pr=10, Sc = 1$ and $Nb = 0.1$.

	Present results	Present results	Khan and Pop [30]	
Nt	$-\theta'(0)$	$-\phi'(0)$	$-\theta'(0)$	$-\phi'(0)$
0.1	0.9524	2.1294	0.9524	2.1294
0.2	0.6932	2.2732	0.6932	2.2740
0.3	0.5201	2.5286	0.5201	2.5286
0.4	0.4026	2.7952	0.4026	2.7952
0.5	0.3211	3.0351	0.3211	3.0351

For the sake of validation, in Table 1, we have made comparisons of existing available literature and limiting case of our model for various values of emerging parameters.

Figures 2-5 demonstrate the fluctuation of velocity profile, angular velocity profile, temperature profile and concentration profiles variation upon magnetic parameter for both assisting and opposing flow. Figure 2 demonstrates that Lorentz force, which decreases the velocity profile for both assisting and opposing flows, causes resistance in the path of fluid flow because of the influence of the magnetic field. The impact of magnetic numbers upon angular velocity is seen in Figure 3. This is evident that larger values of magnetic numbers may lower angular velocity profile for both assisting and opposing flows. In Figure 4, It has been observed that increasing values of M correspond to increasing temperatures distributions. Higher values of M produce a resistive type of force on the motion, reacting in the reverse direction of motion and decreasing the velocity field as a result. The fluid motion simultaneously produced some thermal energy, increasing the fluid temperature for assisting and opposing flows. Figure 5 illustrates the effect of magnetic number upon concentration profile and variation in magnetic number may affect both solutions as a result concentration profile is observed to decrease as M rises.

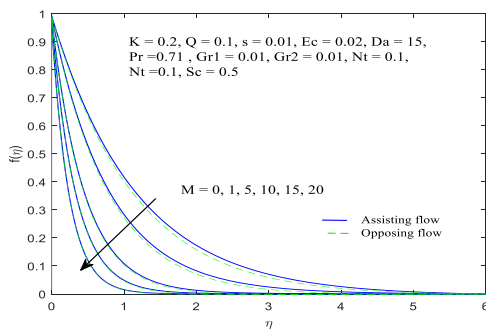


Figure 2: Effects of magnetic number M on Velocity profile.

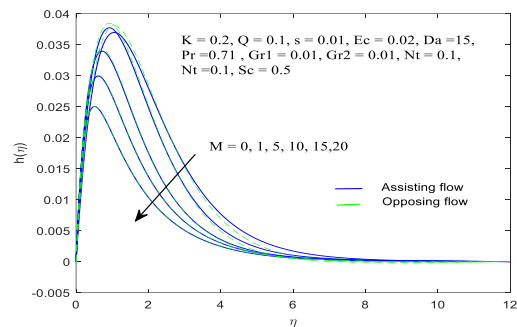


Figure 3: Effects of magnetic number M on Angular velocity profile.

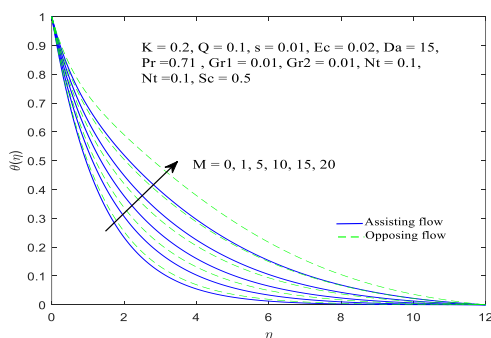


Figure 4: Effects of magnetic number M on temperature profile.

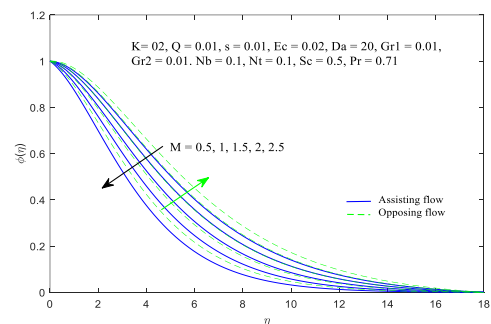


Figure 5: Effects of magnetic number M on concentration profile.

Figures 6-9, Show that changes in the material parameter cause changes in the velocity profile, angular velocity profile, temperature profile, and concentration profile. Figures 6 and 7 illustrate that K varies with velocity and angular velocity profile, respectively. As a result, angular velocity and velocity are increased for assisting and opposing flows and Figures 8 and 9 show the reverse behavior.

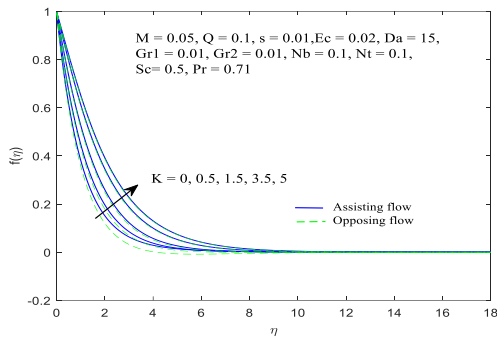


Figure 6: Effects of material number K on velocity profile.

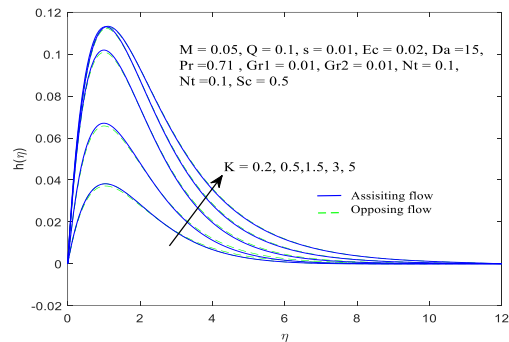


Figure 7: Effects of material number K on Angular velocity profile.

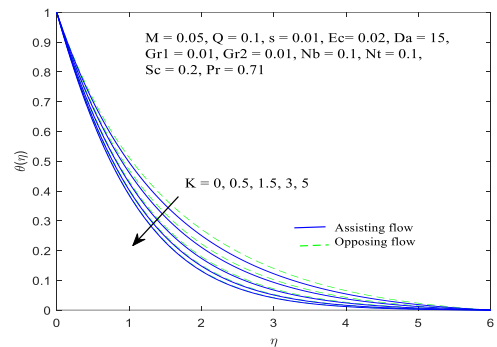


Figure 8: Effects of material number K on Temperature profile.

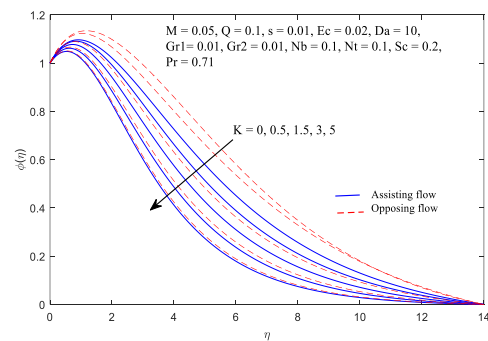


Figure 9: Effects of material number K on Concentration profile

The temperature profile and concentration profile decrease as K increases. Figure 10 shows the fluctuation of the temperature profile examined for Prandtl numbers. The curves clearly show that the increase in Pr causes a lower in temperature. Figure 11 demonstrates that raising Eckert number Ec leads to a decline in temperature on both assisting and opposing flows. Figure 12 illustrates the impact of Schmidt numbers upon concentration profile, the curves show that as Schmidt numbers increase, the concentration profile becomes lower. Figure 13 represents the variation in the concentration profiles of Nt . For assisting and opposing flows, concentration rises as the thermophoresis parameter increases and decreasing for the values of the Brownian motion increase.

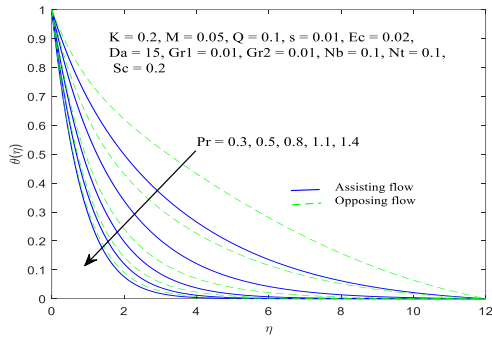


Figure 10: Effects of Prandtl number Pr on Temperature profile.

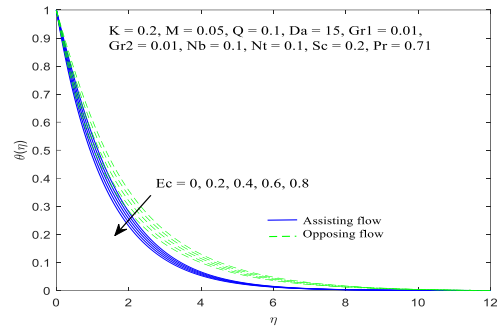


Figure 11: Effects of Eckert number Ec on Temperature profile.

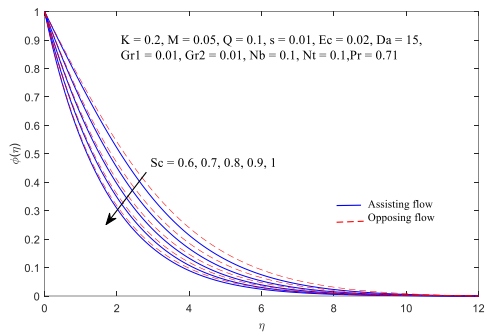


Figure 12: Variation of Sc on Concentration profile.

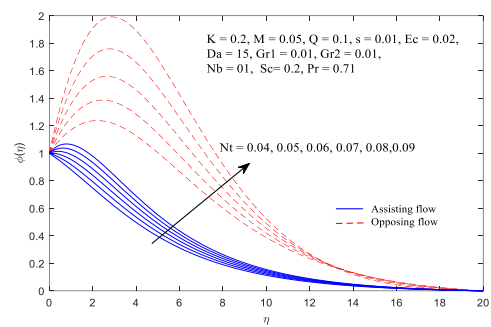


Figure 13: Variation of Nt on Concentration profile.

Figures 14-19 depict the variations in skin-friction, the Nusselt number and the Sherwood number for different values of Eckert number, magnetic number, Brownian motion number, thermophoresis parameter, microrotation and Schmidt number. Figures 14-19 show a variation in the Sherwood number and the Nusselt number, but no change shown for the skin friction because these parameters do not appear in the momentum equation. However, there are some fluctuations in the Sherwood number, but Nusselt number retain its position for these emerging parameters. Figure 19 indicates the slight change in skin-friction along with Sherwood number and Nusselt number.

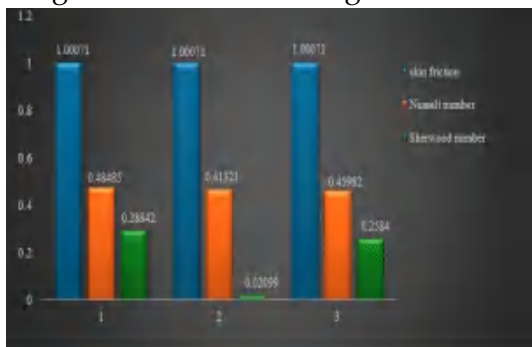


Figure 14: Variation in skin-friction, Nusselt number and Sherwood number for various values of M.

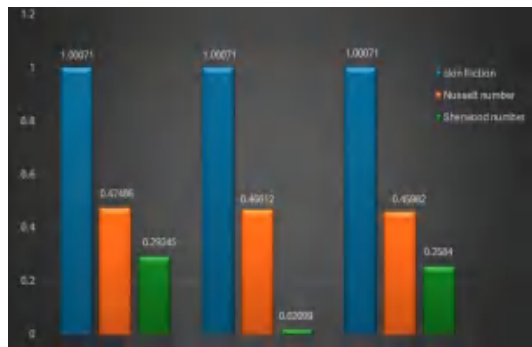


Figure 15: Variation in skin-friction, Nusselt number and Sherwood number for various values of Ec.

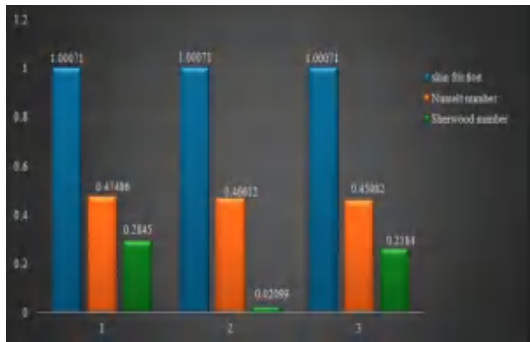


Figure 16: Variation in skin-friction, Nusselt number and Sherwood number for various values of Nb.



Figure 17: Variation in skin-friction, Nusselt number and Sherwood number for various values of Nb.



Figure 18: Variation in skin-friction, Nusselt number and Sherwood number for various values of Nb.

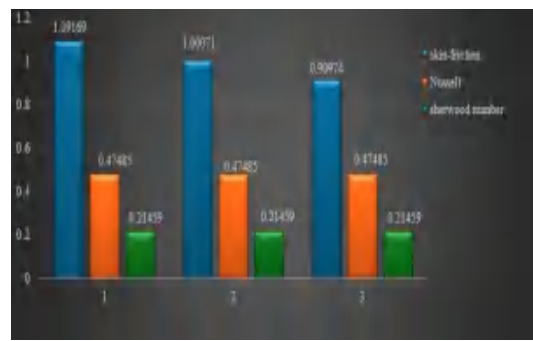


Figure 19: Variation in skin-friction, Nusselt number and Sherwood number for various values of Sc.

5 Conclusions

Based upon the entire results, the following findings are established:

- Higher values of magnetic parameters will decrease the flow field profile, angular velocity and concentration profile for both assisting and opposing flow whereas temperature profile remain low.
- It has been observed that for assisting and opposing flows, the effects of the physical parameter K in the values of the velocities, temperatures, and concentration profiles are opposite of that of the magnetic field parameter.
- Higher numbers of Pr have a greater influence on heat transfer since the Prandtl number rises with temperature.
- As Eckert number increases, the temperature effect also increases. Therefore, with higher values of Ec, their heat transfer properties are enhanced.
- Increasing Schmidt numbers lowers the dimensionless concentration distributions.

- The dimensionless concentration distributions and thermophoresis parameters are increasing.
- Brownian motion parameters are increasing whereas the dimensionless concentration profiles are decreasing.
- Skin friction does not change with increasing values of magnetic number, Eckert number, thermophoresis parameter, Brownian motion parameter, Schmidt number, or micro-rotation, however for higher values of magnetic number, Nusselt and Sherwood numbers are also rising.

Conflicts of Interest

The authors declare no conflict of interest.

References

- [1] A. C. Eringen, Simple microfluids, *Int. J. Eng. Sci.*, 1964, 2(2): 205–217.
- [2] A. C. Eringen, Theory of Micropolar Continua, In: E. Kröner (eds) *Mechanics of Generalized Continua*, 1968. IUTAM Symposia. Springer, Berlin, Heidelberg.
- [3] A. C. Eringen, Theory of micropolar fluids, *J. Math. Mech.*, 1966, 16(1): 1–18.
- [4] T. Ariman, M. A. Turk, N. D. Sylvester, Micro-continuum Fluid Mechanics, A Review, *Int. J. Eng. Sci.*, 1973, 11: 905–930.
- [5] T. Ariman, M. A. Turk, N. D. Sylvester, Application of Micro-continuum Fluid Mechanics, *Int. J. Eng. Sci.*, 1974, 12: 273–293.
- [6] M. A. Turk, T. Ariman, N. D. Sylvester, On Pulsatile Blood Flow, *Trans. Soc. Rheol.*, 1973, 17: 1–21.
- [7] M. A. Turk, T. Ariman, N. D. Sylvester, On Steady and Pulsatile Flow of Blood, *J. Appl. Mech.*, 1974, 41: 1–17.
- [8] H. A. Hogen, M. Hensiksen, An Elevation of a Micropolar Model for Blood Flow Through an Idealized Stenosis, *J. Biomech.*, 1989, 22: 211–218.
- [9] J. D. Lee, A. C. Eringen, Wave Propagation in Nematic Liquid Crystals, *J. Chem. Phys.*, 1971, 54: 5027–5034.
- [10] A. Tozeren, R. Skalak, Micropolar Fluids as Models for Suspensions of Rigid Spheres, *Int. J. Eng. Sci.*, 1977, 15: 511–523.
- [11] S. J. Allen, K. A. Kline, Lubrication Theory of Micropolar Fluids, *J. Appl. Mech.*, 1971, 38: 646–650.
- [12] T. W. Chapman, G. L. Bauer, Stagnation-point viscous flow of an incompressible fluid between porous plates with uniform blowing, *Appl. Sci. Res.*, 1975, 31: 223–239.
- [13] R. S. Agarwal, C. Dhanapal, Stagnation point micropolar fluid flow between porous discs with uniform blowing, *Int. J. Eng. Sci.*, 1988, 26: 293–300.
- [14] H. S. Takhar, V. M. Soundalgekar, Flow and heat transfer of a Micropolar Fluid Past a Porous Plate, *Indian J. Pure Appl.*, 1985, 16(5): 552–558.
- [15] S. K. Jena, M. N. Mathur, Similarity Solutions for Laminar Free Convective Flow of

- Thermomicropolar Fluid Past a Non-isothermal Vertical Flat Plate, *Int. J. Eng. Sci.*, 1981, 19: 1431–1439.
- [16] S. R. Kasiviswanathan, M. V. Gandhi, A class of exact solutions for the magnetohydrodynamic flow of a micropolar fluid, *Int. J. Eng. Sci.*, 1992, 30(4): 409–417.
- [17] H. Lange, The existence of in stationary flows of incompressible micropolar fluids, *Arch. Mech.*, 1977, 29(5): 741–744.
- [18] G. S. Guram, A. C. Smith, Stagnation flows of micropolar fluids with strong and weak interactions, *Comput. Math. Appl.*, 1980, 6: 213–233.
- [19] S. A. Al-Sanea, Mixed convection heat transfer along a continuously moving heated vertical plate with suction or injection, *Int. J. Heat Mass Transfer*, 2004, 47: 1445–1465.
- [20] M. Kumari, G. Nath, Mixed convection boundary layer flow over thin vertical cylinder with localized injection/suction and cooling/heating, *Int. J. Heat Mass Transfer*, 2004, 47: 969–976.
- [21] C. Y. Wang, *Phys. Fluids*, 1988, 31: 466–468.
- [22] M. Sajid, T. Hayat, The application of homotopy analysis method for MHD viscous flow due to a shrinking sheet, *Chaos Solitons Fractals*, 2009, 39: 1317–1323.
- [23] M. Sajid, T. Hayat, T. Javed, MHD rotating flow of a viscous fluid over a shrinking surface, *Nonlinear Dyn.*, 2008, 51(1-2): 259–265.
- [24] S. Liao, A new branch of solutions of boundary-layer flows over an impermeable stretched plate, *Int. J. Heat Mass Transfer*, 2005, 48(12), 2529–2539.
- [25] K. Vajravelu, Viscous flow over a nonlinearly stretching sheet, *Appl. Math. Comput.*, 2001, 124(3): 281–288.
- [26] R. Tsai, K. H. Huang, J. S. Huang, Flow and heat transfer over an unsteady stretching surface with non-uniform heat source, *Int. Commun. Heat Mass Transfer*, 2008, 35(10): 1340–1343.
- [27] A. Ishak, R. Nazar, I. Pop, Uniform suction/blowing effect on flow and heat transfer due to a stretching cylinder, *Appl. Math. Model.*, 2008, 32: 2059–2066.
- [28] C. Y. Wang, Stagnation flow towards a shrinking sheet, *Int. J. Non-Linear Mech.*, 2008, 43: 377–382.
- [29] T. Fang, J. Zhang, Closed-Form exact solutions of MHD viscous flow over a shrinking sheet, *Commun. Nonlinear Sci. Numer. Simul.*, 2009, 14: 2853–2857.
- [30] W. A. Khan, I. Pop, Boundary-layer flow of a nanofluid past a stretching sheet, *Int. J. Heat Mass Transfer*, 2010, 53: 2477–2483.
- [31] M. M. Rahman, M. J. Uddin, A. Aziz, Effects of variable electric conductivity and non-uniform heat source (or sink) on convective micropolar fluid flow along an inclined flat plate with surface heat flux, *Int. J. Therm. Sci.*, 2009, 48: 2331–2340.
- [32] T. Hayat, T. Javed, Z. Abbas, MHD flow of a micropolar fluid near a stagnation-point towards a non-linear stretching surface, *Nonlinear Anal. Real World Appl.*, 2009, 10: 1514–1526.
- [33] A. Ishak, R. Nazar, I. Pop, Magnetohydrodynamic (MHD) flow of a micropolar fluid towards a stagnation point on a vertical surface, *Comput. Math. Appl.*, 2008, 56: 3188–3194.
- [34] A. Ishak, R. Nazar, I. Pop, MHD boundary-layer flow of a micropolar fluid past a wedge with constant wall heat flux, *Commun. Nonlinear Sci. Numer. Simul.*, 2009, 14: 109–118.
- [35] A. Ishak, R. Nazar, I. Pop, Dual solutions in mixed convection boundary layer flow of micropolar fluids, *Commun. Nonlinear Sci. Numer. Simul.*, 2009, 14: 1324–1333.
- [36] T. M. A. El-Mistikawy, Limiting behavior of micropolar flow due to a linearly stretching porous sheet, *Eur. J. Mech. B/Fluids*, 2009, 28: 253–258.
- [37] V. Kumaran, A. K. Banerjee, A. Vanav Kumar, K. Vajravelu, MHD flow past a stretching permeable sheet, *Appl. Math. Comput.*, 2009, 210: 26–32.

- [38] R. Nazar, N. Amin, D. Filip, I. Pop, Stagnation point flow of a micropolar fluid towards a Stretching sheet, *Int. J. Non-Linear Mech.*, 2004, 39: 1227–1235.
- [39] N. F. M. Noor, R. U. Haq, S. Nadeem et al., Mixed convection stagnation flow of a micropolar nanofluid along a vertically stretching surface with slip effects, *Meccanica*, 2015, 50: 2007–2022.

Disclaimer/Publisher's Note: The statements, opinions and data contained in all publications are solely those of the individual author(s) and contributor(s) and not of Global Science Press and/or the editor(s). Global Science Press and/or the editor(s) disclaim responsibility for any injury to people or property resulting from any ideas, methods, instructions or products referred to in the content.